

Target/Moderator options for Powder Diffraction at the ESS

Paolo G. Radaelli – ISIS

I. EXECUTIVE SUMMARY

I have completed a preliminary analysis of the target/moderator options of the powder diffraction programme at the ESS. This includes a series of analytical simulations of steady-state and time-of-flight instruments, and is aimed at addressing the following questions:

1. What is the perspective gain factor at the ESS with respect to existing steady-state and time-of-flight instrumentation?
 2. What is the likely choice of target for the different applications?
 3. What is the likely choice of moderator for the different applications?
 4. What priorities for further moderator developments can be identified?
 5. What are the remaining issues to be addressed by further work?
- Answer to Question 1.: at the ESS we can expect a source-related gain factor varying between 10 and 80 with respect to present-day state-of-the-art instruments. The bigger gains, which can be further increased ($\times 2$) by beam-optics optimisation, are for the longer wavelengths, while the gains at shorter wavelengths are limited by the lack of a truly sharp cold moderator.
 - Answer to Question 2.: all the ESS powder diffractometers should have the 50 Hz target as first choice. Locating some or all the instruments on the 10 Hz short-pulse target will result in a significant but not catastrophic loss in flexibility. Of course, this statement holds true only assuming that there is no peak flux gain in optimising the 10 Hz target over the 50 Hz target. The best instruments to be assigned to the 16.5 Hz long-pulse target are a variable-resolution cold-neutron diffractometer. A Fourier diffractometer can also be considered.
 - Answer to Question 3: coupled moderators are not ideal for powder diffraction, primarily because of the long “tails”. From this provisional assessment, the following moderator choices have emerged:
 - De-coupled poisoned H₂ moderator for high-resolution applications.
 - De-coupled unpoisoned H₂ moderator for medium-resolution magnetic and low-Q diffraction.
 - De-coupled unpoisoned H₂O moderator for medium-resolution crystallography.
 - Answer to Question 4: a truly sharp cold moderator, similar to the ISIS liquid CH₄ moderator, is dearly missed. Some more work should be done to identify a possible alternative.
 - Answer to Question 5: further development work should include:
 - An evaluation of “novel” beam transport systems, especially for medium-resolution crystallography.
 - A quantitative comparison of the long-pulse and short-pulse diffractometers.
 - An evaluation of the potential of a Fourier diffractometer.

II. INTRODUCTION

By all accounts, the outlook for powder diffraction at the new high-power sources in Europe and elsewhere is extraordinarily bright. Powder diffractometers at present pulsed sources are already competitive with steady-state machines, and one can expect further gains of 1-2 orders of magnitude at the ESS. Nevertheless, one can already identify two main challenges for powder diffraction at future high-power pulsed sources. First of all, there is a general desire to broaden the scope of time-of-flight powder diffraction into traditional steady-state strongholds, such as magnetic diffraction. This is in line with the stated philosophy of turning ESS into a “super-ILL” as well as a “super-ISIS”. Secondly, we will have to adapt to a target-moderator landscape bearing little resemblance with the one we have been used to at ISIS and other pulsed sources. This document is a preliminary attempt to address these issues. I have purposely chosen to use rather simple simulation tools, so that a sizeable number of options could be tested. I have also included suggestions for further work to be undertaken in the powder diffraction task group and in the moderator/target group.

III. PRELIMINARY CONSIDERATIONS

Performances of a powder diffractometer

Powder diffraction is in many ways an ideal technique to be applied at pulsed sources. In fact, powder diffraction fulfils the two main criteria for pulse source efficiency: it can make effective use of a broad wavelength band and it benefits from high resolution. In the next few paragraphs we will elaborate on this statement, and set out the fundamental formulas to evaluate the performances of a time-of-flight diffractometer and to compare it with a steady-state diffractometer.

The main difference between steady-state and pulsed sources is that, for the latter, the neutron emission is concentrated in short bursts. In other words, the *peak power* of pulsed sources is much higher than their *average power*. One is primarily interested in maximising the time-averaged flux on the sample. In fact, the average count rate for a diffractometer

$$P \propto F \cdot O_{\text{det}} \cdot \mathbf{e}_{\text{det}} \cdot V_{\text{eff}}, \quad (1)$$

is proportional to the time-averaged flux on the sample, the detector solid angle and the “effective” (absorption-corrected) sample volume.

Under certain circumstances, however, the source parameter that ultimately determines the instrument count rate is in fact the *peak power*. For a diffractometer, this is verified when the following two conditions are simultaneously met:

1. The pulse width is a significant component of the resolution function.
2. The time frame (i.e., the range of time-of-flights in which “useful” neutrons are collected) is equal to the reciprocal of the source repetition rate. We will see later that this condition dictates the wavelength band to be employed by the diffractometer.

If condition 2. Is verified, it is possible to show that the average flux on the sample for a pulsed-source diffractometer is given by

$$\bar{F} = R \cdot \langle B_{\text{peak}}(\mathbf{l}) \cdot \mathbf{e}(\mathbf{l}) \cdot \Omega_{\text{source}}(\mathbf{l}) \rangle, \quad (2)$$

where $B_{\text{peak}}(\mathbf{l})$ is the peak *brilliance* (neutrons·sec⁻¹·cm⁻²·sterad⁻¹·%BW⁻¹), R is the dispersive ($\Delta\tau/\tau$) component of the resolution (here assumed to be constant), $\mathbf{e}(\mathbf{l})$ is the optical system efficiency and $\Omega_{\text{source}}(\mathbf{l})$ is the viewing solid angle of the source (moderator or guide; in the latter case the solid angle is wavelength-dependent)¹. The average is over the wavelengths used by the instrument. Equation (2) has to be compared with the equivalent formula for a steady-state source,

$$F = R \cdot B_{\text{peak}}(\mathbf{l}) \cdot \mathbf{e}(\mathbf{l}) \cdot \Omega_{\text{source}}(\mathbf{l}), \quad (3)$$

where, now, $R = \mathbf{Dl}/l^2$. The comparison between equations (2) and (3), taking into account equation (1) as well, elicits a few considerations:

- Steady-state sources can optimise the peak brilliance by choosing the optimum wavelength (usually near the Maxwellian peak). On the contrary, broad-bandwidth time-of-flight machines are penalised by the averaging over a wide range of wavelengths away from the peak.

¹ Equations (2) and (3) are strictly true for a triangular peak. For a different shape, there is an additional peak form factor $f(\mathbf{l})$ that is equal to $(\mathbf{p}/4\ln 2)^{1/2} = 1.06$ for a Gaussian and $1/\ln 2 = 1.443$ for an exponential. Since the latter gain is all in the tail, it can be ignored. For practical purposes we will assume $f(\mathbf{l}) = 1$.

² When the diffractometer employs chromatic (horizontal) focussing, R is the bandwidth for a small element of the monochromator surface, since the focussing effect is accounted for by the monochromator solid angle $\Omega_{\text{source}}(\mathbf{l})$.

- The viewing solid angle of the source is a very important optimisation parameter in both cases. One is interested in maximising W_{source} without degrading the resolution of the instrument. In steady-state diffractometers, this is usually accomplished through focussing monochromators, which combine vertical and horizontal (chromatic) focussing. This results in relatively large W_{source} ($\sim 5 \times 10^{-4}$ sterad), whilst preserving an ultimate resolution of the order of $R = DI/I$. On the contrary, the tendency of time-of-flight machines has been to set the maximum source divergence (both vertical and horizontal) to be comparable to the sample-detector divergence, resulting in a factor of 10 *smaller* values of W_{source} .
- The smaller source solid angle of time-of-flight diffractometers is more than compensated by the much larger *detector* solid angles (up to a factor of 40 for comparable machines) typically available at ISIS pulsed diffractometers, due to both engineering and funding considerations.
- Since ISIS and the ILL have comparable peak brilliances, and all the other factors in Equation (1) balance out in the first approximation, comparable machines at the two sources should have comparable performances. For the two high-resolution machines D2B and HRPD, which have overlapping domains of application, this has been empirically demonstrated through the experience of many users. The same is not true for high-flux machines, which are optimised for rather different uses at the two sources.

The wavelength bandwidth of a time-of-flight diffractometer

As already mentioned, the wavelength band is a critically important parameter defining the performances of a time-of-flight diffractometer. Its maximum value is defined by the need to avoid *frame overlap*, which is the superposition of neutrons coming from different pulses onto the same frame:

$$\Delta I_{Max} (\text{\AA}) = \frac{3957}{n_{source} \cdot L_{tot} (m)}, \quad (4)$$

where n_{source} is the repetition rate of the source and L_{tot} is the total flight-path.

It is important to distinguish between this *single-frame* bandwidth and the effective bandwidth, which can be much larger if multi-frame data acquisition is employed (see below) In modern time-of-flight diffractometers, this single-frame wavelength band is usually set by means of a system of choppers. It is immediately apparent from (4) that long instrument at fast sources have a narrow bandwidth. When this is perceived to be a disadvantage, another chopper can be added to reduce the source frequency by suppressing some of the pulses. Another approach is that of making repeated measurements with different wavelength ranges. This is known as *multi-frame* data collection.

Resolution of a time-of-flight diffractometer

In addition to the usual geometrical terms, the pulse width usually gives an important contribution to the instrumental resolution, especially in back scattering. The actual shape of the pulse and its dependence on wavelengths are complex functions, dictated by the physical processes occurring within the

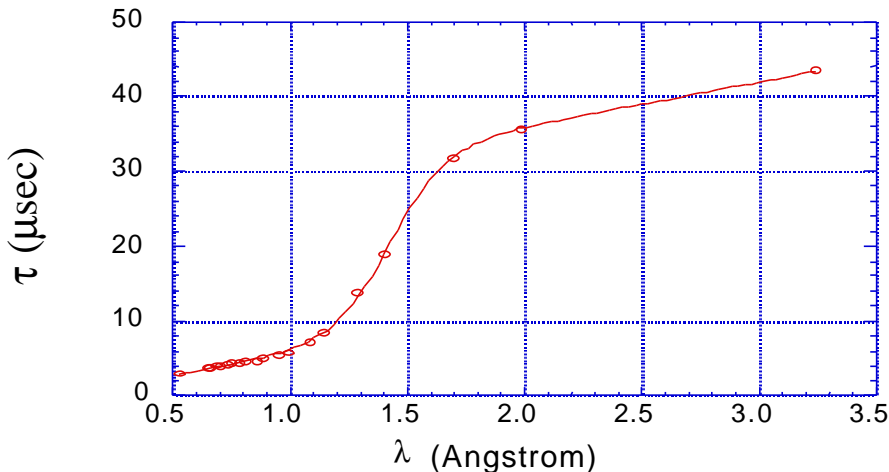


Figure 1: Exponential decay constant for the ISIS liquid-methane moderator, measured on GEM.

moderator¹(Figure 1). Quite often, it is assumed that Dt is directly proportional to I , which would be equivalent to approximate the curve in Figure 1 with a straight line with zero intercept, and, in this case, and approximate slope $S \sim 1 \cdot 10^{-5} \text{ sec}/\text{\AA}$. The pulse-width component of the resolution function can then be approximated by

$$R_{pulse} \approx \frac{3956}{L_{tot} (m)} \cdot \Sigma \quad (5)$$

Combining (4) with (5) we obtain:

$$\Delta I_{Max} (\text{\AA}) = \frac{R_{pulse}}{n_{source} \cdot \Sigma}, \quad (6)$$

which defines the relationship between bandwidth, resolution, repetition rate and pulse width.

Setting the optimum bandwidth-first and second-generation instruments

At the end of the seventies, when the first time-of-flight diffractometers were being conceived for pulsed sources such as Zing-P', IPNS, and, later, ISIS, a number of options were considered in principle. However, at the end, the design philosophy was dictated by considerations of mostly practical nature:

- The need to avoid as much as possible expensive neutron guides favoured relatively short instruments ($L_{tot} \sim 10\text{-}15 \text{ m}$). Because of equation (5), good resolution could only be obtained with small S . This dictated the use of “sharp” (decoupled/poisoned) water or cold (liquid or solid) methane moderators.
- Because of equation (4), relatively broad bandwidths ($>6 \text{ \AA}$) could be obtained even at high repetition rates (50-60 Hz). One added cost-saving advantage of this is the ability to run without choppers.
- The original methods of time-of-flight data reduction (electronic focussing) and analysis (single-histogram Rietveld refinement) also favoured broad bandwidths, which allowed relatively large wavelength-dispersive histograms to be produced.
- Although recognised in principle very early on, multi-frame data collections, whereby data collected with a number of chopper phases are merged to yield a single extended histogram, have developed rather slowly, and are currently applied only at cold-neutron time-of-flight diffractometers such as IRIS and OSIRIS at ISIS. Once again, the reason for this is the need for powerful computers and sophisticated software to merge and correct multi-frame data.

The only first-generation instrument that departed radically from this design philosophy was HRPD at ISIS. Here, the goal to attain a resolution of 4×10^{-4} imposed the use of a long flight path (95 m) and of a curved neutron guide. Nevertheless, HRPD routinely operates with a relative large bandwidth (4 \AA), thanks to a frame-suppressing chopper rotating at 10 Hz. Once again, this yields a wide enough frame on the back-scattering detector (typically $0.5 \text{ \AA} < d < 2.5 \text{ \AA}$) to be analysed in isolation, and still be useful for most crystal chemical problems.

Setting the optimum bandwidth-third generation instruments

It is clear that most of the considerations underpinning the design philosophy of first-generation diffractometers are now superseded by developments in neutron optics and by the massive increase of computing power available to the instrument scientists and the users. For example, multi-histogram analysis of time-of-flight data from different detector banks, once performed only in exceptional circumstances, is now applied routinely, automatically and, to a certain extent, transparently, on instruments such as GEM². Also, merging of multi-frame data on HRPD is performed more and more often to double or treble the single-frame d-spacing range. In the near future, and certainly well before the advent of the ESS, new data collection techniques, such as commensurate or incommensurate chopper “slewing” will enable narrow-bandwidth instruments to perform extended data collections as short as a few frames. Consequently, the single-frame bandwidth is rapidly losing importance as a defining parameter for diffractometers design. This provides the designer with a much greater flexibility on the choice of moderator-target packages, and significantly broadens the scope of time-of-flight powder diffraction

techniques, in particular, towards traditionally underdeveloped areas such as medium-resolution magnetic diffraction. In the remainder, we will assume that these technical developments will have come to full fruition by the commencement of the ESS interment design *stricto sensu*. We will also assume that the growth in the available computing power will not have slowed down significantly in the intervening time. On the basis of this, we can make the following general considerations:

- As for steady-state diffractometers, the most important instrument-defining parameters are the operating wavelength(s) and the resolution. The single-frame bandwidth is, as a first approximation, a “free” parameter.
- Other critical parameters being equal, it can be argued that, with few exceptions, narrow-bandwidth instruments are more flexible than broad-bandwidth ones. In fact they can be operated as wavelength-dispersive (by slewing the choppers), quasi-angle-dispersive or even for looking at single Bragg peaks with high intensity. However, narrow-bandwidth instruments are also more complex and more expensive, because they require sophisticated chopper systems and a long guide. While this is basically unavoidable for high-resolution machines, we can foresee some psychological resistance to going this route for medium-resolution machines. This is one of the main issues to be debated before finalising the choice of the target-moderator packages.
- The main exception to the previous statements occurs when hot neutrons (with wavelengths significantly below 1 Å) are required. These wavelengths cannot be easily transported with existing guide systems, consequently forcing relatively small flight-paths and hence wider bandwidths. In this case, the choice of flight-path will be largely dictated by the available moderator areas and by the possible development of new (ballistic) guide systems. In modern powder diffraction, there is a recognised tendency towards using higher-Q data, which needs to be fostered at new high-power sources.
- A broad single-frame bandwidth is also required for single-pulse, wavelength-dispersive measurements. We note that single pulse measurements (with 20 msec time resolution) are entirely within the realm of possibilities for high-intensity diffractometers at the ESS.

IV. COMPARISON WITH EXISTING INSTRUMENT/SOURCES

In this section, I will attempt to make a quantitative comparison between existing state-of-the-art instrumentation at steady-state and pulsed sources and at the ESS. It is important to remark that, in doing this, I will not introduce any element of novelty in the instrumentation itself, but I will only consider the enhanced performances of the source. Any technical advances, such as substantial enhancement of detection efficiency at short wavelengths, will presumably apply to old and new sources alike, and will not alter the results of the comparison. A completely different issue, which we will not discuss here, is whether current sources are fully exploited based on present-day technology.

Choosing the instruments for the comparison

It seems appropriate to base the comparison on the most recent instrumentation installed at existing sources. For both ILL and ISIS, the latest powder diffractometers are both high-intensity, medium-resolution machines, D20 and GEM, respectively. D20 became operational in 1997, while GEM saw its first neutrons in late 1999. As already remarked, these medium-resolution machines have quite different characteristics, which reflect the differences in scientific interests of the ILL and ISIS powder diffraction communities. In the most commonly used configuration, D20 has a resolution $Dd/d \approx 0.01$, and achieves a high count rate mainly through high flux on the sample. These characteristics are ideal for studying magnetic diffraction and the macroscopic parameters (lattice parameters, phase fractions, peak intensities, etc.) of time-resolved chemical or physical phenomena. On the contrary, GEM has a much better resolution $Dd/d \approx 0.002$, and a much lower incident flux, which is compensated by a very large detector solid angle. This is ideal to study both macroscopic and microscopic parameters (atomic coordinates, Debye-Waller factors, occupancies, etc.) with a very high time resolution. Because of these differences, the comparison between these instruments has to be taken *cum grano salis*. As for the ESS, I have taken an instrument with the same characteristics of GEM (flight-path, detector system, moderator size) and tested it on 4 different *de-coupled* moderators (cold-poisoned, cold-unpoisoned, thermal poisoned, thermal-

unpoisoned). Clearly, using a coupled moderator at 17m primary flight-path is not a viable option, and I have not considered it here.

Defining the parameters for the comparison

I will present comparisons between two different parameters. The first one is the *effective flux* f_{eff} , which enables one to calculate the integrated intensity I_{hkl} of a given Bragg peak, expressed in neutrons per second:

$$I_{hkl} [n/ sec] = F_{eff} \times \frac{V_{sample} \cdot f}{v_{u.c.}} \times m_{hkl} |F_{hkl}|^2, \quad (7)$$

where V_{sample} is the sample volume in cm^3 , $v_{u.c.}$ is the unit cell volume in Ångstroms, f is the packing fraction of the powder, m_{hkl} is the reflection multiplicity and $|F_{hkl}|^2$ is the square of the structure factors expressed in Barns. Perhaps a better indicator of relative performances for instruments with different resolution (see below) is the *effective peak height* H_{eff} , which is given by the effective flux divided by the peak width (FWHM) in Ångstroms.

$$H_{eff} = \frac{F_{eff}}{W[\text{Å}]} \quad (8)$$

The expression used to calculate the peak widths (resolutions) and the two performance indicators from the source/moderator parameters will be included in a future draft of this document. The instrument parameters used for the simulations are summarised in Table I. The resolution curves for the six instruments are plotted in Figure 2.

Table I: Instrument characteristics for the comparative simulations of steady-state and time-of-flight diffractometers at present sources and at the ESS.

	Monochromator /Moderator	Flux/Incident spectrum	Flight-paths L_1/L_2	Detector system	Efficiency
D20	HOPG 42° take-off, 2.4 Å	3.7×10^7 n/cm ² /sec [†]	-	³ He microstrip system, 1600 elements.	90%
GEM	ISIS CH ₄ poisoned	From V-rod measurements	17m/1.3-2.3m	6 banks of SZn scintillators, 8000 elements, $W_{det} = 3.5$ sterad	50% @ 1 Å
ESS-1	H ₂ decoupled poisoned	From ESS-Instr.-4.12.00	17m/1.3-2.3m	6 banks of SZn scintillators, 8000 elements, $W_{det} = 3.5$ sterad	50% @ 1 Å
ESS-2	H ₂ decoupled unpoisoned	From ESS-Instr.-4.12.00	17m/1.3-2.3m	6 banks of SZn scintillators, 8000 elements, $W_{det} = 3.5$ sterad	50% @ 1 Å
ESS-3	H ₂ O decoupled poisoned	From ESS-Instr.-4.12.00	17m/1.3-2.3m	6 banks of SZn scintillators, 8000 elements, $W_{det} = 3.5$ sterad	50% @ 1 Å
ESS-4	H ₂ O decoupled unpoisoned	From ESS-Instr.-4.12.00	17m/1.3-2.3m	6 banks of SZn scintillators, 8000 elements, $W_{det} = 3.5$ sterad	50% @ 1 Å

[†] Source: ILL-D20 web page.

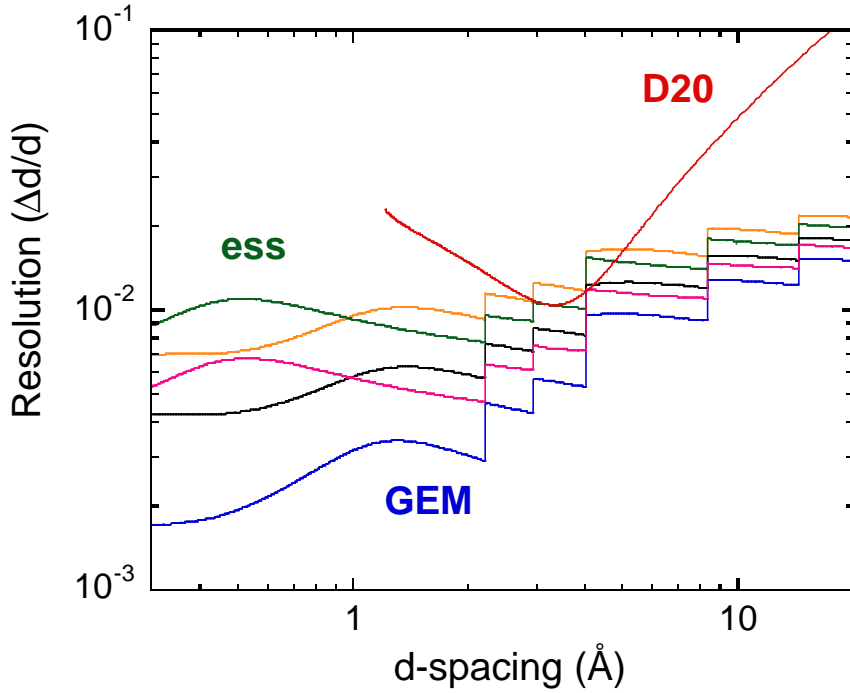


Figure 2: Resolution functions of GEM (blue), D20 (red) and GEM-like instruments at ESS on the 4 decoupled moderators: H₂-poisoned (black), H₂-unpoisoned (orange), H₂O-poisoned (light gray) and H₂O-unpoisoned (dark gray).

The first thing to notice is the quite considerable loss of resolution of the ESS instruments with respect to GEM, the primary flight-path being equal. This is due, on one hand, to the poorer peak-shape characteristics of the ESS-H₂ moderators with respect to the ISIS-CH₄ moderator, and to the fact that the switch-over between slowing-down and thermalisation occurs at much shorter wavelengths for H₂O than for either H₂ or CH₄. It is noteworthy that the resolution functions of the ESS instrument are still below that of D20 in the high-flux configuration used here. Nevertheless, a realistic analogue of GEM at the ESS will have to be moved farther away from the moderator, at or beyond 40 m (more on this later). Part of the loss in source solid angle W_{source} can be compensated by the large surface area of the ESS moderators (120×120 mm²: here, we have used the canonical ISIS value of 100×100 mm²). Even larger moderators (e.g., 140×140mm²) would be worth considering, if technically feasible, since the loss of resolution is likely to be a problem common to other instruments.

The effective flux and effective peak height parameters, f_{eff} and H_{eff} , for the same set of instruments are plotted in Figures 3 and 4, respectively. f_{eff} is the relevant parameter when the sample contribution to the resolution function dominates the instrumental term, or when one is interested in determining integrated intensities from data with poor statistics. H_{eff} is the parameter used in most data collection strategies (which generally look at signal-to-noise ratios) for samples that are well matched to the instrument. Even if all Bragg peaks are resolved, an increase of the peak width at constant H_{eff} will somewhat improve the statistics on the structure factors but will worsen the accuracy on lattice parameters and propagation vectors. Obviously, a decrease of the peak width is an advantage for partially overlapping peaks. It is clear from the data that we can expect an improvement of over two orders of magnitude in both f_{eff} and H_{eff} at long d spacing with respect to GEM. The improvement over D20 is over an order of magnitude for f_{eff} and two orders of magnitude for H_{eff} . At first sight, these numbers may appear excessive by a factor of 2-4,

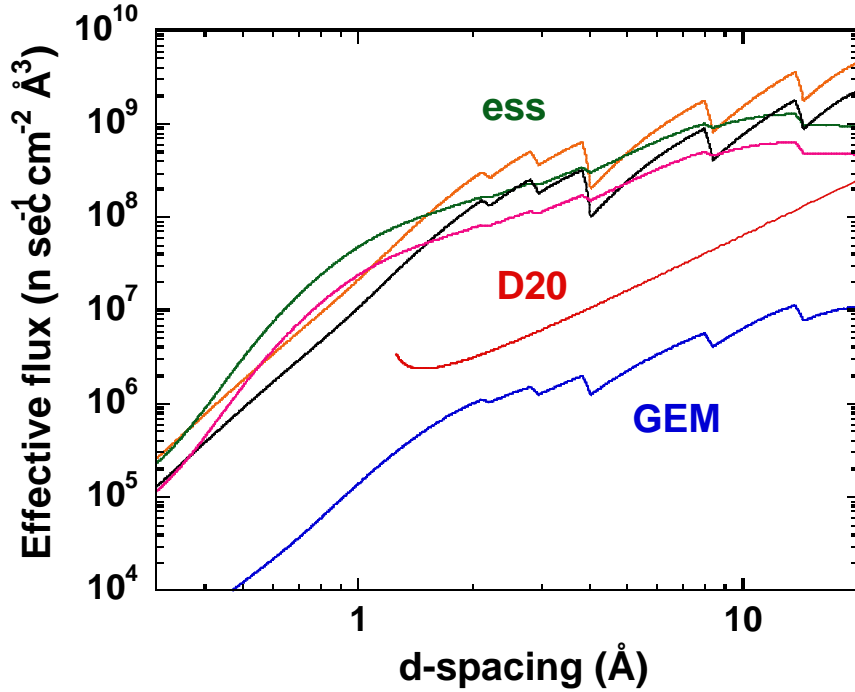


Figure 3: Effective flux parameter f_{eff} (see text) for GEM (blue), D20 (red) and GEM-like instruments at ESS on the 4 decoupled moderators: H₂-poisoned (black), H₂-unpoisoned (orange), H₂O-poisoned (light gray) and H₂O-unpoisoned (dark gray).

considering that the peak brilliance of the will only be 30 times that of ISIS or of the ILL. However, one has to consider the following:

- When normalised to the respective peak brilliances, ESS moderators yield 2-4 times broader peaks with respect to ISIS. This directly translates in higher f_{eff} , and will also increase H_{eff} at long d , where the pulse-width contribution to the resolution function is small.
- There appears to be an additional gain in peak brilliance over the tightly-poisoned CH₄ moderator of ISIS.

V. THE PROPOSED ESS INSTRUMENT SUITE

The original suite of ESS instruments³ included 6 powder diffractometers (see Table II). Two of them were located on the 50 Hz target and 4 on the 10Hz target. 5 out of 6 diffractometers were assigned to high-resolution cold moderators, while the remaining one (15-m high-intensity diffractometer) was assigned to the thermal high-resolution moderator. In considering this suite of instruments, one can make the following comments:

- The assignment of the high-resolution ($Dd/d \sim 1 \cdot 10^{-3}$) and ultra-high-resolution ($Dd/d \sim 5 \cdot 10^{-4}$) diffractometers to the poisoned H₂ moderator cannot be called into question. On the basis of the curves in Figure 2, we can estimated the primary flight-paths of these two machines to be ~ 100 and ~ 200 m, respectively. There is no penalty in moving these two instrument to the 50 Hz target, which has some added advantages. First of all, it enables a novel single-peak ($Dd \sim 0.2 \text{ \AA} @ 200 \text{ m}$), high-intensity mode of operation. Although this scheme is probably more useful for single crystal diffraction, it has been employed successfully in the past at synchrotron sources, and could be very appealing for the physical crystallography community. Secondly, data collected at 50 Hz could be easily focussed into a single histogram in angle-dispersive mode⁴ ($DI \sim 0.4 \text{ \AA} @ 200 \text{ m}$). These

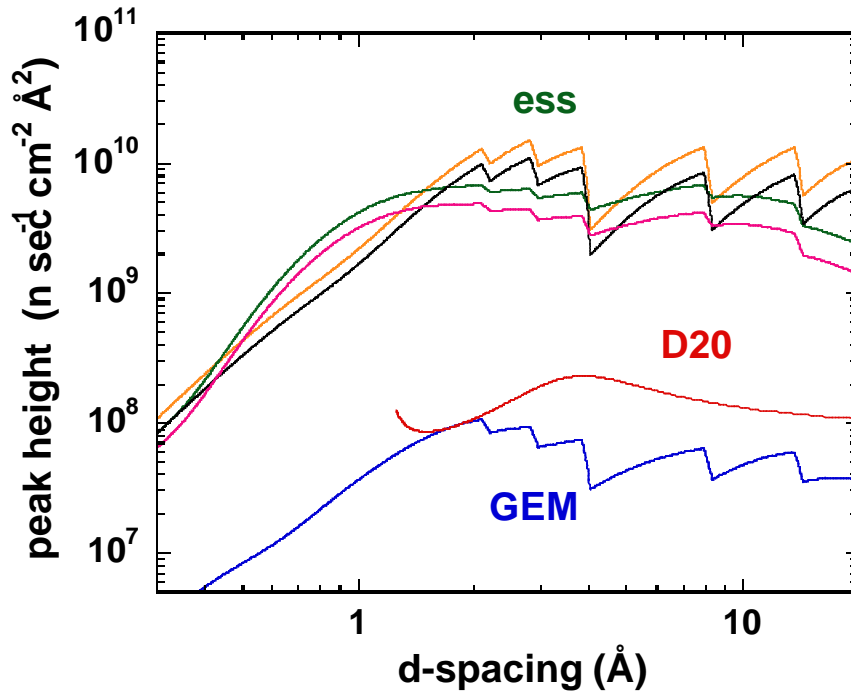


Figure 4: Effective peak height parameter H_{eff} (see text) for GEM (blue), D20 (red) and GEM-like instruments at ESS on the 4 decoupled moderators: H_2 -poisoned (black), H_2 -unpoisoned (orange), H_2O -poisoned (light gray) and H_2O -unpoisoned (dark gray).

data are expected to have a better signal-to-noise ratio and to be easier to analyse than wavelength-dispersive data. Clearly, low-frequency operation, or, equivalently, high-frequency multi-frame data collection, would still be available to collect “conventional” wavelength-dispersive data. We will later remark that the proposed long-pulse target is an amenable location for a high-resolution powder diffractometer.

Table II: Reference suite of powder diffractometers, for the European Spallation Source Study³, Volume III, pp 5-3, 5-4.

Target Station 1 High Frequency 50 Hz				Target Station 2 Low Frequency 10 Hz			
Ambient High Resolution Moderator		Cold High Resolution Moderator		Cold High Intensity Moderator		Cold High Resolution Moderator	
High-Intensity Powder Diffractometer	15 m	High-Pressure Powder Diffractometer	12 m			High-Resolution Powder Diffractometer	75 m + guide
						Ultra High-Resolution Powder Diffractometer	150 m + guide
						Polarised High-Intensity Powder Diffractometer	10 m
						Magnetic Powder Diffractometer	50 m + guide

- As we have already seen, and will see in more detail later on, single-pulse data collection on gram-size samples will be possible at relatively good resolutions ($Dd/d \sim 2-3 \cdot 10^{-3}$). Consequently, one should

thoroughly probe the scientific case for any powder diffractometer shorter than 40m. Also, 12m for a high-pressure machine may not be enough, considering the recent progress in laser-heating techniques to remove pressure-induced broadening.

- Most notably, the proposed instrument suite lacks a medium-resolution machine ($Dd/d \sim 1-2 \cdot 10^{-3}$) with access to considerable epithermal flux. This clearly contradicts the recent trend to exploit high-Q data, either with Rietveld refinements or with Fourier-transform methods. I will discuss later the possible choice of moderators for this application. I will anticipate, however, that a 40m instrument looking at a poisoned H₂O moderator appears to be the likely choice, unless new sophisticated beam transport techniques can be implemented.
- Magnetic powder diffraction is the most likely candidate for the use of unpoisoned moderators. Here, the loss of epithermal neutrons due to the longer primary flight path is not a severe problem, and the loss is compensated by the gain in peak brilliance of the moderator. Being a “typical” physical crystallography application, magnetic diffraction will almost certainly benefit from the 50 Hz operation, as explained above. Similar considerations are valid for a possible high-pressure magnetic diffractometer.
- Coupled moderators are not considered viable for powder diffraction. In fact, they would force unreasonably long flight paths, and produce undesirable tails that cannot be cut effectively, due to the polychromatic nature of time-of-flight diffraction.

VI. THE CHOICE OF THE TARGET/MODERATOR PACKAGE: INSTRUMENT SIMULATIONS

Instrument parameters

In defining the choice of the target/moderator package, one has to take into account three fundamental parameters:

1. The combination of moderator type and primary flight path, which defines the ultimate resolution of the diffractometer.
2. The source/chopper setting, which defines the average value of the wavelength and its single-frame range.
3. The detector configuration and the data collection strategy, which defines the Q-range of the measurement and the Q-dependent resolution function., as well as the fragmentation of the data set.

In this preliminary analysis of the problem, I have considered in detail points 1. and 2., making the assumption that data collected at all scattering angles will be of use. I plan to make a more complete assessment of the impact of the detector design and the data collection strategy in the final version of this document. I have chosen to consider an instrument with a peak resolution $Dd/d \sim 2 \cdot 10^{-3}$. As already discussed, this resolution can be reached by at least two different viable choices of the moderator and primary flight-path.

Methods

I have compared two medium-resolution ESS instruments with comparable resolution $Dd/d \sim 2 \cdot 10^{-3}$: a 40m machine looking at a poisoned H₂ or H₂O moderator and an 80m machine looking at an unpoisoned H₂ or H₂O moderator. As a reference, I have also calculated the performances of a 17-m ISIS machine looking at a poisoned CH₄ moderator, also having a similar resolution. The detector system I have chosen is the same in all cases: a continuous detector with a secondary flight path of 2m and a constant elevation angle of $\pm 22.5^\circ$ on either side of the equatorial plane, for a total solid angle of \mathbf{p} . All the calculations were performed analytically, using the moderator parameters given in the document ESS-Instr.-4.12.00. The following beam line parameters were adopted:

- For the 17m-ISIS instrument, the sample has a direct view of a 100×100mm² CH₄ moderator, without any guide.

- For the 40m ESS instrument on the poisoned moderators, the first 20m of the flight tube, which has the same dimensions as the moderator ($120 \times 120 \text{ mm}^2$), is coated in Ni ($g = 0.00173 \text{ rad/\AA}$) on all 4 sides, while the rest of the flight tube is coated with an absorber.
- For the 80m ESS instrument on the unpoisoned moderators, the first 76.6m of the flight tube, which is straight and has dimensions $20 \times 40 \text{ mm}^2$, are coated with Ni on all 4 sides.

It is noteworthy that the maximum vertical divergence of the 80m machine is doubled with respect to the other two. Therefore, we can expect a factor of two gain in effective flux. The 40m instrument could be equally optimised by adding a guide section coated on the top and bottom sides. This option was not considered here, as it introduces an additional complication in the simulation.

A simple analytical expression, based on the calculation of the number of “bounces” at a given divergence angle, was used to calculate the guide transmission. Since the difference in instrument resolution between the different configurations is quite small, I have chosen to compare the values of f_{eff} . The ESS curves have been normalised to the ISIS curve, to yield a wavelength-dependent “gain factor”. The ISIS 17m instrument was operating at 50 Hz, with a wavelength band of 4.05 \AA . All the parameters used in the simulation are summarised in Table III.

Wide-band operation

The gain factors of the two ESS instruments operating in wide-band mode (25 Hz for the 40m machine and 10 Hz for the 80m one) are shown in Figure 5 for both H_2 and H_2O moderators. For the cold moderators, one can immediately observe that the gain for the 40m ESS diffractometer over the 17m ISIS one is a factor of 50 at long d-spacings, while the gain is less than a factor of 10 below 0.5 \AA . As already observed, the fundamental reason for this is the poorer resolution of the H_2 poisoned moderator with respect to the ISIS CH_4 one, which forces to double the flight-path and, consequently, to have a 4-times smaller direct view of the moderator. We already commented on the fact that the long-wavelength gain is more than the canonical factor of 30. The 80m instrument is better by another factor of 3.6 at long wavelengths. Of this, a factor of 2 is due to the optimised optics. A good part of the rest is due to the higher peak flux from the unpoisoned moderator. However, the short-wavelength performances are significantly deteriorated. This would suggest that the 40m machine is better suited for high-Q crystallographic applications, while the 80m diffractometer is better for magnetism. The gain curves are somewhat more balanced for the water moderators. An H_2O moderator could perhaps be adopted for the 40m machine, if the scientific programme calls for predominantly crystallographic work (this choice was done at the SNS for the 80-m POW-GEN3). Further changes could be introduced by adopting a more efficient optical system (e.g., a ^{58}Ni guide or even a ballistic guide).

Table III: Instrument characteristics for the comparative simulations of different target/moderator choices at the ESS.

	Monochromator /Moderator	Flight-paths L_1/L_2	Beam optics system	Operating Frequencies
ISIS-17m	ISIS CH_4 poisoned	17m/2m	Direct view of $100 \times 100 \text{ mm}^2$ moderator.	50 Hz
ESS-40m- H_2	H_2 decoupled poisoned	40m/2m	20 m of $120 \times 120 \text{ mm}^2$ Ni guide.	25 Hz 50 Hz
ESS-40m- H_2O	H_2O decoupled poisoned	40m/2m	20 m of $120 \times 120 \text{ mm}^2$ Ni guide	25 Hz
ESS-80m- H_2	H_2 decoupled unpoisoned	80m/2m	76.6 m of $20 \times 40 \text{ mm}^2$ Ni guide	10 Hz 25 Hz 50 Hz
ESS-80m- H_2O	H_2O decoupled unpoisoned	80m/2m	76.6 m of $20 \times 40 \text{ mm}^2$ Ni guide	10 Hz

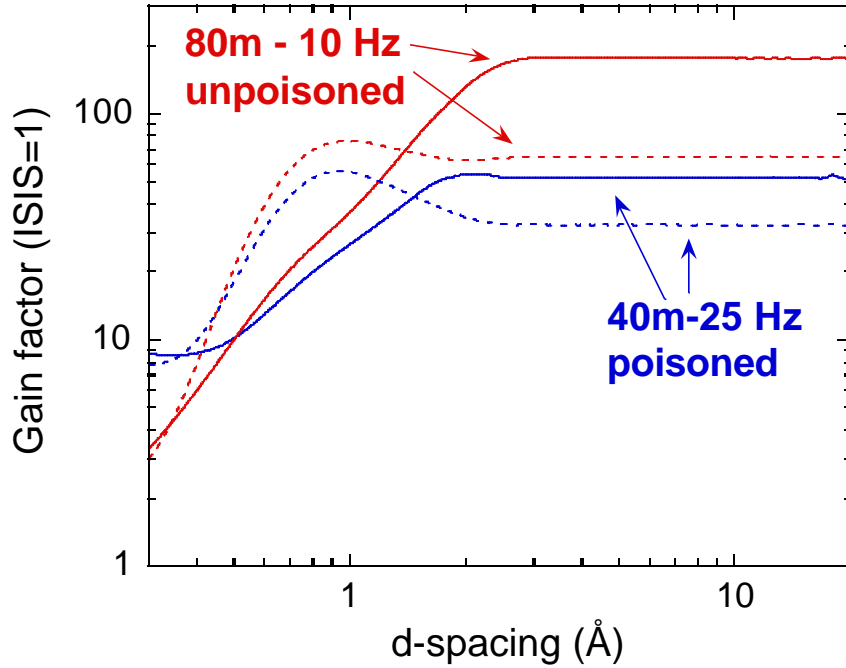


Figure 5: Effective flux gain factors over an equivalent ISIS machine for two ESS medium-resolution diffractometers: a 40m machine looking at a poisoned H_2 moderator (blue continuous line) and a poisoned H_2O moderator (blue dotted line) and for an 80m machine looking at an unpoisoned H_2 moderator (red continuous line) and an unpoisoned H_2O moderator (red dotted line).

Frequency-dependent gains

Figures 6 and 7 show the effect of varying the operating frequency (and hence the single-frame bandwidth) for the 40m and the 80m diffractometers, respectively.

By all accounts, high-frequency operation is particularly appealing when one is only interested in d-spacing above 1 \AA . In this case, a gain of a factor of two over the wide-band operation is attainable. We can also draw another interesting conclusion from Figure 7: at 80 m, there is no longer any gain from going from 25 to 50 Hz. This happens because we are effectively in the angle-dispersive limit, where the wavelength spread contributes little to the Q-range. Of course, this will no longer be true if one looks at a narrow angular range, for instance, in back scattering, to achieve high resolution. In this approach, one can still trade Q-range for flux.

VII. PERSPECTIVES AT A LONG-PULSE TARGET

The long 2.5 msec pulse from the proposed long-pulse target is not suitable as such for powder diffraction use, and needs to be reshaped. This is done by means of a disc chopper placed at a distance L_{chop} from the moderator. It is easy to deduce the following relationship between L_{chop} , the pulse length t and the band width:

$$\Delta I \text{ (\AA)} = \frac{3956}{L_{chop}} \cdot t, \quad (9)$$

40 metres

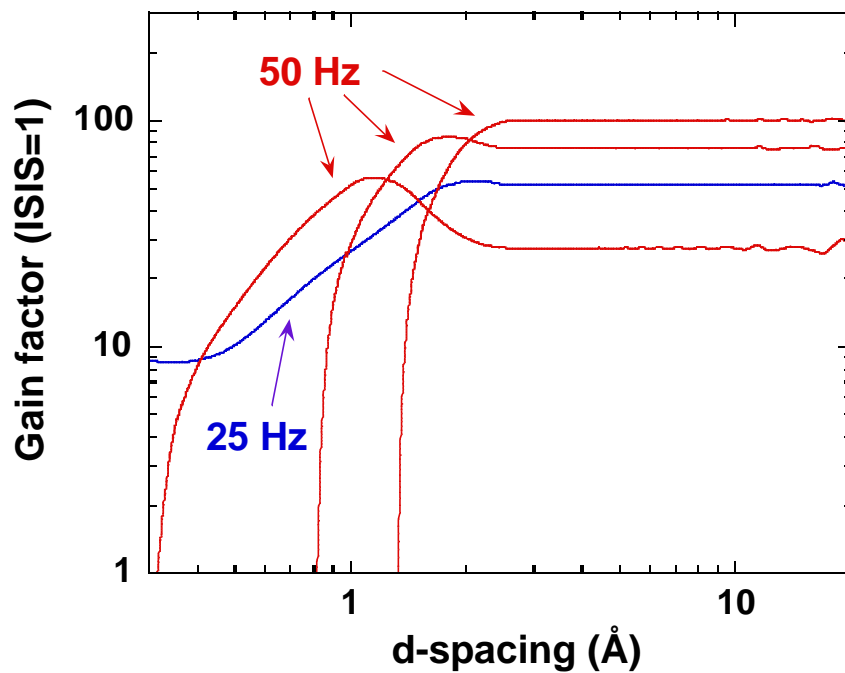


Figure 6: Effective flux gain factors as a function of the operating frequency over an equivalent ISIS machine for the 40m ESS medium-resolution diffractometer. The blue curve is for 25 Hz operation, while the red curves are for 50 Hz with wavelength bands centred at 1.5, 2.5 and 3.5Å

80 metres

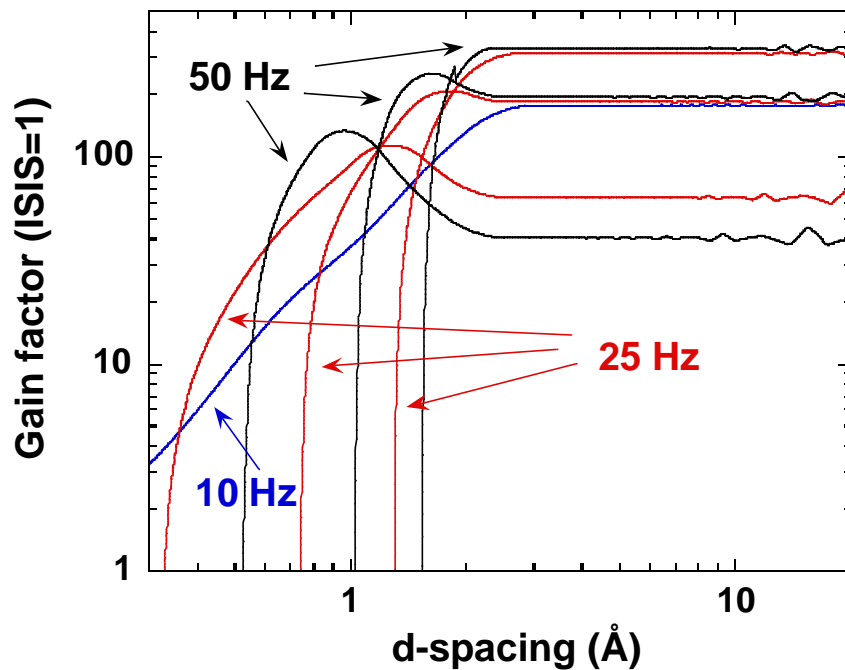


Figure 7: Effective flux gain factors as a function of the operating frequency over an equivalent ISIS machine for the 80m ESS medium-resolution diffractometer. The blue curve is for 10 Hz operation. The red and black curves are for 25 Hz and 50 Hz, with wavelength bands centred at 1.5, 2.5 and 3.5Å.

Taking $L_{chop} = 6$ m (slightly less than the standard ISIS value of 6.5 m), and $t = 2.0$ msec (we here consider only the intense part of the pulse) one calculates a band width of 1.28 Å. From equation (4), one can then calculate the primary flight path at which the resulting histogram is filled, which is also the condition for optimum use of the peak brilliance.

$$L_{tot} = \frac{L_{chop}}{n \cdot t}, \quad (10)$$

from which one deduces a flight path of 181 m at 16.5 Hz. The most favourable application for such a source/moderator combination would be for a cold-neutron, variable-resolution diffractometer⁵, with excellent peak resolution and perfectly triangular peak shape. At long wavelengths, the long-pulse target peak-brilliance compares more favourably with the short-pulse targets. Also, at long wavelengths, the chopper system is better optimised (for chopper-shaped pulses, for any given bandwidth, there is a penalty factor $\sim \frac{I_{min}}{I_{max}}$ on the peak brilliance). Possible applications are for the study of extended magnetic

defects and for complex structure solution. Nevertheless, the peak brilliance loss is a factor of two at best over the short-pulse target for the wavelengths of interest, and it is hard to argue for this machine as a first choice. Because of the predictable pressure on the 50 Hz target, this option should be considered as a very strong possibility should the long-pulse target replace the original 10 Hz target.

A possible alternative would be a high-resolution Fourier diffractometer⁶, of the type that successfully operated for a long time at the IBR-2 reactor in Dubna. A much broader bandwidth (and consequently shorter) machine could be viable, and state-of-the-art electronics and computing technique should make the data reduction and analysis much more facile than in the past. We will investigate this option in greater detail in a future draft of this document.

VIII. FINAL CONSIDERATIONS

Preliminary assessments

From this analysis of the target/moderator options for powder diffraction at the ESS, it is possible to make some preliminary statements, which, in my view, are unlikely to change after a more careful investigation.

- Given the choice, the 50 Hz target is always better than the 10 Hz one. However, locating a number of instruments on the 10 Hz target would only result in a rather minor loss in flexibility.
- The poisoned de-coupled H₂O and unpoisoned de-coupled H₂ moderators are the likely first choices for structural and magnetic work, respectively. At high resolution, the poisoned H₂ moderator is ideal for both fields.
- We dearly miss a truly sharp cold moderator, especially for crystallography requiring high and low Q at the same time. Perhaps, one should look more closely at hybrid moderators.
- The long-pulse target is an unlikely first choice for powder diffraction. However, if it is built, a cold variable-resolution diffractometer and a Fourier diffractometer should be considered as the most promising choices.

General considerations

To conclude this analysis, some more general considerations are in order. If the choice of abandoning the 10 Hz target is made, this would result in an enormous pressure onto the 50 Hz target. Most likely, of the instruments originally assigned to the 10 Hz target, only 50% or less will have the long-pulse target as their first choice. In particular, the 50 Hz target would be the first choice for all the powder (and, probably, single-crystal) diffractometers. Even assuming that some of the instrument originally on the 50 Hz would

shift to the long-pulse target, this is likely to create a problem. In a sense, this is unavoidable, if one's goal is to widen the scientific breath of ESS from being a "super-ISIS" to combining this with a "super-ILL" role. However, the powder diffraction community should be swift in looking after its interests (which, in this scenario, will be threatened) as well as recognising the needs of the broader neutron community.

IX. REFERENCES

- ¹ S. Ikeda and J. M. Carpenter, Nucl. Instr. and Methods in Phys. Res. **A 239** (1985) 536-544.
- ² W.G. Williams, R.M. Ibberson, P. Day and J.E. Enderby, Physica B **241-243** (1998) 234-236.
- ³ The European Spallation Source Study – Volume III: The ESS Technical Study, ESS-96-53-M, November 1996.
- ⁴ P.G. Radaelli, "Extending the Domain of Time-of-Flight Powder Diffraction Techniques", in *ICANS XIV – Proceedings of the 14th meeting of the International collaboration on Advanced Neutron Sources*, edited by J.M. Carpenter and C.A. Tobin, ANL-98/33, June 1998.
- ⁵ J.A. Stride, D. Wechsler, F. Mezei and H.-J. Bleif, "Powder Diffraction on a Long Pulse Spallation Source, Nucl. Instr. and Methods in Phys. Res. *in Press*.
- ⁶ V.L. Aksenov, A.M. Balagurov and V.A. Trounov, J. Neutron Research **Vol, 6** (1997) 135-148.